

Fig. A The comparison on carbon background signal intensity using epoxy resin and Sn-based alloy.

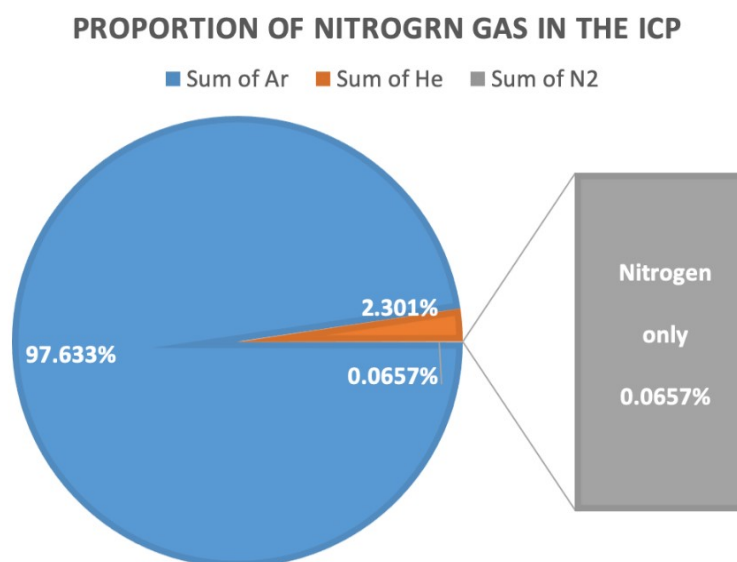


Fig. B Proportion of Nitrogen gas in the ICP

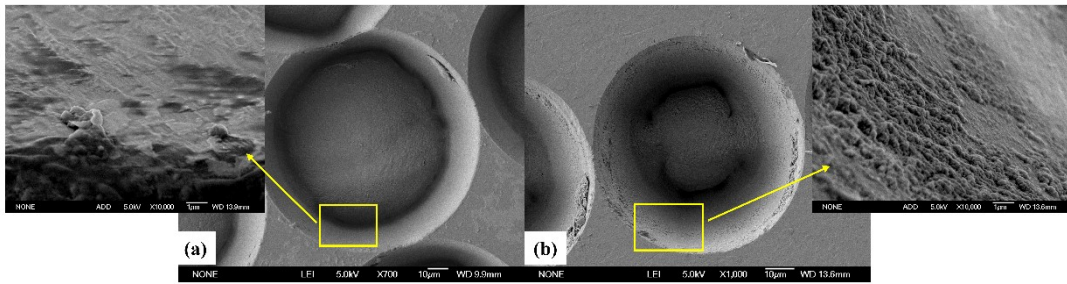


Fig. C The SEM images of the laser holes. (a) The SEM image of the natural diamond. (b) The SEM image of the HTHP diamond.

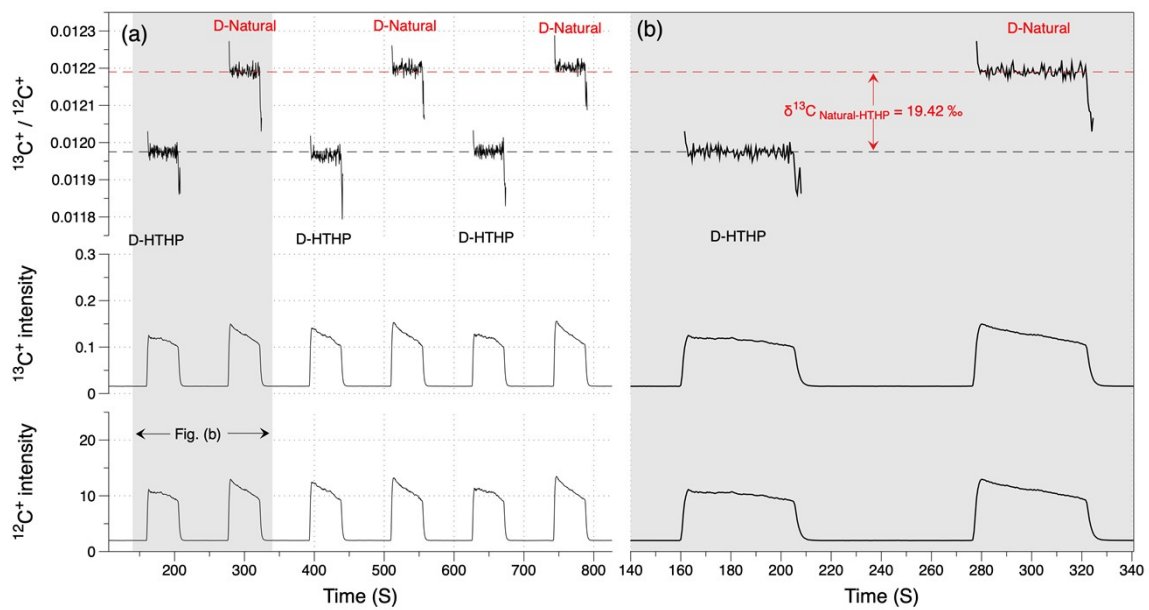


Fig. D TRA data for natural and HTHP diamonds with LA-MC-ICP-MS. Although the signal drift differently for natural and HTHP diamonds, no C-isotope fractionations were found neither in HTHP nor natural diamonds during the laser ablation process. Part of (a) was enlarged in (b).

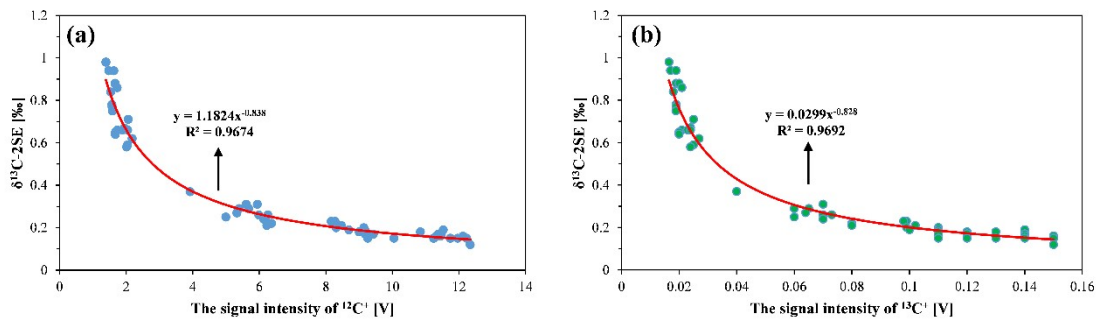


Fig. E The relationship between the internal precision (2SE) of  $\delta^{13}\text{C}$  and the intensities of  $^{12}\text{C}^+$  and  $^{13}\text{C}^+$ . (a): The relationship between the internal precision (2SE) of  $\delta^{13}\text{C}$  and the intensities of  $^{12}\text{C}^+$ ; (b) The relationship between the internal precision (2SE) of  $\delta^{13}\text{C}$  and the intensities of  $^{13}\text{C}^+$ ;

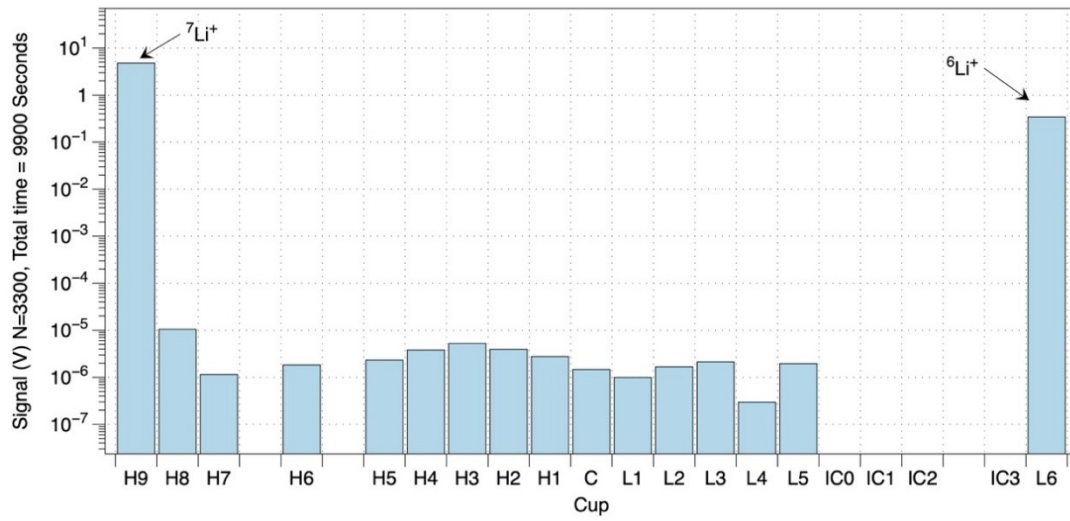


Fig. F Signal intensity of the collectors when measuring Li isotope, no tailing was observed, hence, it is sufficient to separate  ${}^{40}\text{Ar}^{3+}$  from  ${}^{13}\text{C}^+$ .